ELSEVIER

Journal of Hydrology 248 (2001) 14–34

Journal of Hydrology

www.elsevier.com/locate/jhydrol

A multi-tracer study in a shallow aquifer using age dating tracers ^{3}H, ^{85}Kr, CFC-113 and SF_6 — indication for retarded transport of CFC-113

Sebastian Bauer[a,*], Christian Fulda[b], Wolfgang Schäfer[c]

[a]*Department of Applied Geology, Institute of Geology, University of Tübingen, Sigwartstrasse 10, D-72076 Tübingen, Germany*
[b]*Joint Scientific Research Institute (GGA), Stilleweg 2, 30655 Hannover, Germany*
[c]*Interdisciplinary Center for Scientific Computing, University of Heidelberg, Im Neuenheimer Feld 368, 69120 Heidelberg, Germany*

Received 11 August 1998; revised 5 February 2001; accepted 6 March 2001

Abstract

We describe field observations and numerical simulations of the environmental tracers ^{3}H, ^{85}Kr, CFC-113 ($C_2Cl_3F_3$), SF_6 and Ne in groundwater. The field site is a well-characterised shallow aquifer in central Germany, consisting of basalts of Miocene age, overlain by up to 15 m of loess deposits. A two-dimensional numerical model was used to simulate tracer transport at the study site. Simulated and observed tracer concentrations show acceptable agreement for most wells and tracers. Due to the variable thickness of the loess cover, residence times of ^{3}H in the unsaturated zone are highly variable with values ranging from 1 to more than 30 years. This effect explains the observed variability of ^{3}H in the saturated zone. Excess air in groundwater requires correction of measured concentrations of the dissolved gas tracers. A maximum excess of the SF_6 content in water compared to the theoretical solubility equilibrium concentration of 28% was observed. A novel iterative method is used to correct for excess air. CFC-113 transport seems to be retarded. On the basis of the effective porosity for SF_6, ^{85}Kr and ^{3}H transport, a retardation factor of $R = 1.5$ for CFC-113 with respect to SF_6, ^{3}H and ^{85}Kr can be derived. Together with non-adsorbing tracers, such as ^{85}Kr or SF_6, CFC-113 can therefore serve as a reactive retardation tracer exploring mean sorption characteristics of the aquifer material. Extrapolation of CFC-113 sorption characteristics to organic contaminants with comparable physicochemical properties (e.g. chlorinated hydrocarbons) offers an opportunity for improved assessment of the behaviour of this important group of contaminants in groundwater.

Keywords: Groundwater tracer ; Multi-tracer study; Groundwater model; Adsorption

1. Introduction

Observations of piezometric heads together with information on hydraulic properties, such as aquifer thickness and hydraulic conductivity, allow characterisation of the flow system of a given aquifer in terms of specific flux and flow pattern. Frequently, groundwater flow models are used in such studies to obtain quantitative results. However, flow modelling does not directly provide information on flow velocity, because flow velocity is connected to specific flux via the effective porosity. The effective porosity, i.e. the porosity in which tracer transport takes place, is usually smaller than the total geometric porosity of the medium. Whereas the value of the effective porosity is not used in a steady state flow model, it has a significant impact on species transport in

* Corresponding author.
E-mail address: sebastian.bauer@uni-tuebingen.de (S. Bauer).

0022-1694/01/$ - see front matter
PII: S0022-1694(01)00381-X

groundwater, because it determines flow velocities and thus residence times of dissolved species in groundwater. The effective velocity of sorbing substances is further affected by interactions with the aquifer material.

Information on the effective porosity and on sorptive mechanisms in aquifers is an important prerequisite for assessment of groundwater contamination or for selection of remediation strategies. To determine the flow velocity in an aquifer on a regional scale, transient tracers can be used. These are trace substances with a well-known time dependent input into groundwater and well known sinks or sources in the subsurface. Linking observed groundwater concentrations to the known input function might allow the reproduction of the transport history of the tracer and the age dating of a groundwater sample. Examples of global transient tracers are tritium (^{3}H), chlorofluorocarbons (CFCs), krypton-85 (^{85}Kr) and sulfurhexafluoride (SF_6). They all are predominantly of anthropogenic origin and were released into the atmosphere and hydrosphere during the past few decades.

Successful groundwater studies using global transient tracers were conducted, e.g. by Eriksson (1963) (^{3}H), Ekwurzel et al. (1994), Dunkle-Shapiro et al. (1998) (^{3}H/^{3}He), Rózanski and Florkowski (1979), Smethie et al. (1992) (^{85}Kr), Busenberg and Plummer (1992), Oster et al. (1996) (CFCs) and Cook et al. (1995), Katz et al. (1995), Szabo et al. (1996) (CFC-113). An overview of recent transient tracer studies can be found in Cook and Solomon (1997).

Simultaneous measurement of various tracers within multi-tracer studies can significantly enhance the information gained. Differences in water ages determined from different tracers point to either insufficient understanding of the transport processes involved or to missing or inaccurate data on aquifer properties or tracer characteristics (i.e. local input function, recharge rates, degradation or sorption of the tracers). Multi-tracer studies in shallow porous aquifers conducted by Ekwurzel et al. (1994), Cook et al. (1995), Szabo et al. (1996) and Plummer et al. (1998 a,b) have resulted in similar groundwater ages derived from various tracers. In addition, CFC degradation and retardation could be deduced from the combined results from different tracers.

In the study presented here, the transient tracers ^{3}H, ^{85}Kr, CFC-113 and SF_6 were used to study transport mechanisms in a shallow fractured rock aquifer. In addition, concentrations of Ne-isotopes were measured to determine excess air in groundwater.

The multi-tracer study was part of an interdisciplinary project on nitrate reduction in catchment areas of water supply wells initiated by the state of Hessia, Germany. The objective of the tracer study was to determine the characteristic time scale of the shallow aquifer, i.e. the mean residence time of water in the aquifer. The knowledge of this mean residence time is necessary for the prediction of nitrate transport and the response time of the aquifer with regard to nitrate input, i.e. the time that expires before reduced nitrate losses from the top soil will lead to decreased nitrate concentrations in the wells. This contribution is focused on selected aspects of the multi-tracer study while results of the nitrate project are described elsewhere (HMUG, 1996; Zoellmann and Kinzelbach, 1996; Zoellmann et al., 2001).

2. Methods

^{3}H and ^{85}Kr are well-known groundwater age dating tracers, whereas literature about the use of CFC-113 and especially SF_6 as groundwater tracers is still scarce. Therefore, they will be described in more detail.

2.1. Input functions and transport mechanisms of the tracers

^{3}H is the radioactive isotope of hydrogen with a half-life of 12.43 years (Unterweger et al., 1980). There is a low natural ^{3}H background in precipitation of 5–10 TU (Craig and Lal, 1961; Dreisigacker and Roether, 1978; TU denotes Tritium Unit, which equals one atom of ^{3}H per 10^{18} atoms of ^{1}H). Surface and near-surface nuclear weapon testing in the early 60s resulted in very high ^{3}H concentrations in precipitation of up to 8000 TU. Monthly mean winter values of ^{3}H concentrations in precipitation from a representative site at Hof, Germany, approximately 240 km from the field site (monthly measurements, G. Bader, pers. communication), were used to define the input function (Fig. 1). Taking mean winter values assumes that summer recharge, which has higher ^{3}H concentrations, rarely reaches the water table, and

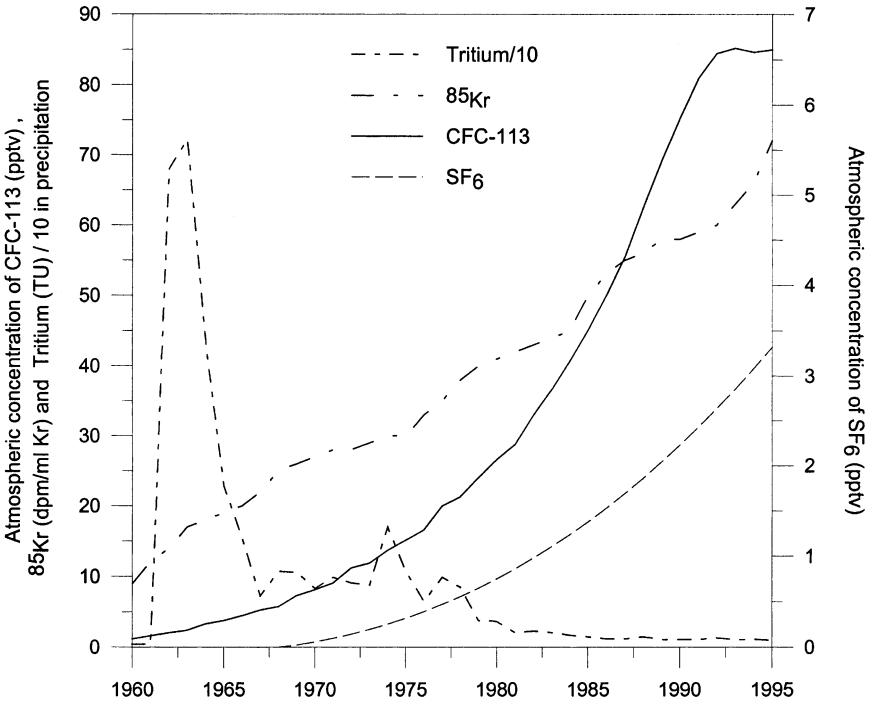

Fig. 1. Mean winter values of ^{3}H (left axis. Multiply by 10 for original values) in precipitation at Hof (Germany). Also shown are the activities of ^{85}Kr in precipitation (left axis) and the atmospheric background concentrations of CFC-113 (left axis) and SF_6 (right axis).

therefore the ^{3}H input function thus defined may slightly underestimate the ^{3}H input. Measurements at Hof reach back to 1962. Before 1962 the atmospheric background concentration is estimated, since there are no continuous measurements available for Central Europe. This means that in our approach we neglect some of the ^{3}H from the late 1950s, but ^{3}H concentrations were much lower than in the early 1960s. The ^{3}H input function is the same as the one used by Zoellmann et al., (2001).

^{85}Kr is a radioactive isotope of the noble gas krypton with a half-life of 10.76 years (Seelmann-Eggebert et al., 1981). A low natural background concentration of ^{85}Kr is produced by spallation and (n, γ) reactions of cosmic neutrons with the stable isotope ^{84}Kr. Almost all ^{85}Kr in the environment is of anthropogenic origin, mainly produced during nuclear weapon testing, in nuclear reactors and in nuclear reprocessing plants. It is a fission product of uranium and plutonium and ^{85}Kr emission is directly related to plutonium production (Schröder and Roether, 1975). The atmospheric concentration of ^{85}Kr has been documented by Sittkus and Stockburger (1976), Rózanski and Florkowski (1979), Rath (1988) and Weiss et al. (1992). As ^{85}Kr concentrations are recorded in terms of specific activity, i.e. the ratio of ^{85}Kr to stable Kr of a sample (in disintegrations per minute of ^{85}Kr per normal millilitre of Kr, dpm cm^{-3} STP), groundwater age evaluation by this tracer is not affected by solubility or recharge temperature (Smethie et al., 1992). For the same reason excess air (discussion of excess air see below) does not affect the age evaluation (Cook and Solomon, 1997). The specific activity of ^{85}Kr in the atmosphere used in this study (Fig. 1) is taken from DVWK (1995) and is consistent with other published values for the mid latitudes of the northern hemisphere (e.g. Weiss et al., 1992).

CFC-113 (CCl_2FCClF_2) is an anthropogenic compound with no known natural sources. It is mainly used as cooling and cleaning agent, especially in the electronics industry, from where it is released to the atmosphere. Its atmospheric lifetime is about 85 a (Fraser et al., 1996). CFC-113 acts as a greenhouse

gas (Dickinson and Cicerone, 1986) and contributes to ozone depletion by photolytic processes in the stratosphere (Molina and Rowland, 1974). Therefore, release of CFC-113 to the atmosphere was restricted by the Montreal Protocol (WMO, 1988) and emission of CFC-113 is prohibited in the industrialised countries since January 1996.

Measurements of atmospheric CFC-113 concentrations were reported by Singh et al. (1977, 1983), Tominaga (1992) and Simmonds et al. (1992). Fraser et al. (1996) provide an extensive summary of tropospheric CFC-113 measurements in clean air. In this study the atmospheric background concentrations from Mace Head, Ireland and Cape Meares, Oregon, USA, were used to reconstruct the atmospheric concentration of CFC-113 over time for maritime clean air at mid latitudes of the northern hemisphere (data from Fraser et al., 1996; Montzka et al., 1996; see Fig. 1). Prior to 1978 no measurements are available and the atmospheric concentration of CFC-113 had to be extrapolated backward in time. It is assumed that CFC-113 emissions increased exponentially from 1960 to 1980 (AFEAS, 1996). Therefore, an exponential function was used to reconstruct the temporal evolution of atmospheric CFC-113 concentration prior to 1978. Due to the restrictions in the Montreal Treaties, atmospheric concentrations of CFC-113 reached their maximum in 1993 and have been nearly constant since then (Montzka et al., 1996; Hurst et al., 1997). This trend is corroborated by own unpublished air measurements performed at Heidelberg during spring 1997, which provided a mean atmospheric CFC-113 concentration of 86 ± 1.6 pptv (1 pptv is 1 part per trillion of volume $= 10^{-12}$ (cm^3 STP CFC-113)(cm^3 STP air)$^{-1}$). Due to the long atmospheric lifetime, atmospheric concentrations of CFC-113 are expected to decrease only slowly.

Solubility of CFC-113 in fresh water and seawater for different temperatures was measured by Bu and Warner (1995). The Bunsen coefficient of CFC-113 for freshwater at a temperature of 10°C is 148 cm^3 STP kg^{-1}. The CFC-113 concentration in maritime air in 1995 (Fig. 1) results thus in a CFC-113 equilibrium concentration in freshwater at 10°C of about 563 fmol l^{-1}.

Transport of CFC-113 in groundwater can be affected by adsorption to the aquifer material. Under the assumption of linear, reversible and instantaneous adsorption, CFC-113 retardation compared to water movement can be described by a constant retardation factor R (e.g. Kinzelbach, 1992)

$$R = 1 + \rho K_D \frac{(1-n)}{n_e}, \quad (1)$$

where ρ is the density of the solid phase, n the total porosity of the medium, n_e the effective porosity and K_D is the solid–liquid partitioning coefficient. R can also be interpreted as the ratio of conservative tracer velocity (^{3}H, ^{85}Kr) to retarded tracer velocity (CFC-113). Under certain conditions K_D may be derived from the organic-carbon–water partitioning coefficient of the compound, K_{OC}, or the octanol–water partitioning coefficient of the compound, K_{OW}, and the fractional organic carbon content of the aquifer material, f_{OC}, using empirical relationships. For trichloroethene Schwarzenbach and Westall (1981) found

$$K_D = f_{OC}\ K_{OC} = 3.09\, f_{OC}\ K_{OW}^{0.72}. \quad (2)$$

Eq. (2) is valid only for $f_{OC} > 0.1\%$, since adsorption on mineral surfaces may become dominant at smaller values of f_{OC} and Eq. (2) may then significantly underestimate partitioning to the solid phase. Adsorption can also be observed in rocks without organic carbon (Haderlein and Schwarzenbach, 1993; Ciccioli et al., 1980).

Experimental evidence of the adsorption of CFC-113 results from column and field experiments. Ciccioli et al. (1980) found no retardation of CFC-113 in columns filled with Ottawa sand, but measured a retardation factor of $R = 1.5$ in columns filled with ground limestone. From their data a partitioning coefficient of $K_D = 0.07$ can be estimated. Jackson et al. (1992) measured a retardation factor of $R = 12$ ($K_D = 1.45$) during passage of CFC-113 through a column filled with Glouster aquifer sediment. This high retardation is probably due to adsorption to mineral surfaces and organic substrates (Jackson et al., 1992). In the aquifer itself Lesage et al. (1990) found the distribution of CFC-113 to be similar to the distribution of PCE, which has a K_{OW} value of $\log K_{OW} = 2.66$($K_D = 0.18$, using $f_{OC} = 0.1\%$). Cook et al. (1995) measured depth profiles of CFC-113, ^{3}H and CFC-12 and determined retardation factors for CFC-113 relative to ^{3}H and CFC-12 of $R = 1.7$ and 1.3, respectively ($K_D = 0.14$ and 0.09).

K_{OW} values of CFC-113 may be estimated using

empirical relationships. Relationships from Schwarzenbach et al. (1993) and the Handbook of Physical and Chemical Parameter Estimation (Lyman et al., 1982) lead to $\log K_{OC} = 2.7$ and 2.8, respectively. A correlation by Sontheimer et al. (1983) gives $\log K_{OC} = 2.65$. Using the solubility of CFC-113 from Bu and Warner (1995) and a relationship from Roy and Griffin (1985) $\log K_{OC} = 2.02$ is obtained. These findings derived from thermodynamic considerations show that adsorption of CFC-113 is likely. However, estimated organic carbon distribution coefficients may only be accurate to within an order of magnitude (Roy and Griffin, 1985).

SF_6 is a gaseous compound under environmental conditions. It is primarily used as an insulating gas in switchgear from which it escapes mainly by leaks (Ko et al., 1993). Further applications are in aluminium and magnesium production (MacNeal et al., 1990; Stordal et al., 1993), in insulating glass and as working gas in leak detectors (Solvay, 1994). SF_6 is mainly of anthropogenic origin (Ko et al., 1993). Recently, a natural production leading to a background concentration of about 0.3% of the atmospheric signal of maritime air in 1995 has been suggested (Harnisch and Eisenhauer, 1998). Because of its infrared adsorption bands (Hertzberg, 1966) and its long atmospheric lifetime (on the order of thousands of years; Ravishankara et al., 1993), SF_6 has an extremely high global warming potential per molecule. However, because atmospheric concentrations are in the range of a few pptv only, the greenhouse effect due to SF_6 is still negligible (Ko et al., 1993; Albritton et al., 1994).

Clean air atmospheric background concentrations of SF_6 are shown in Fig. 1. Measured data from five maritime air stations, covering the period from 1978 to 1995, were used to derive the SF_6 concentration in maritime air in the northern hemisphere (Maiss et al., 1996). These results are in good agreement with results by Geller et al. (1997), who used latitudinal profiles, hourly measurements and archived air to reconstruct the atmospheric SF_6 concentrations as a function of time. The relative deviation from the data of Maiss et al. (1996) is less then 3%.

Solubility measurements of SF_6 in water are reported by Friedman (1954), Morrison and Johnstone (1955) and Ashton et al. (1968). Wilhelm et al. (1977) have used the data from Ashton et al. (1968) to derive an equation based on thermodynamic laws that describes the temperature dependence of the SF_6 solubility in water. The solubility inferred from this equation is in good agreement with the above-mentioned measurements and further data from Gerrard (1980), Watson and Liddicoat (1985) and Wanninkhof et al. (1991). The Bunsen coefficient of SF_6 for freshwater at 10°C is about 10 cm^3 STP kg^{-1}, which means that SF_6 concentration in maritime air in 1995 (Fig. 1) results in a SF_6 equilibrium concentration in water of about 1.5 fmol l^{-1}. This value is low compared to the other trace gases used in this study.

2.2. Continental excess

Long-term records of atmospheric concentrations of SF_6 and CFC-113 are available for clean air monitoring sites only, mainly maritime locations. The stations are usually far away from the source locations of these gases. This implies that concentrations of these two gases are elevated, relative to maritime values, in regions with higher industrial activity. Determination of local excess of anthropogenic trace gases have been published by several groups (Geller et al., 1997 for SF_6; Singh et al., 1977, 1992; Simmonds et al., 1987 for CFC-113). In the present study a simple approach similar to that presented in Oster (1994) is used to estimate local CFC-113 and SF_6 concentrations. It is assumed that the local excess relative to clean air concentration (δ) is proportional to the emission rate $E(t)$ of the trace gas, i.e. that the time dependence of the local excess is the same as of the emission rate. The local air concentration C_A of the trace gas is then given by

$$C_A(t) = C_{A0}(t)(1 + \delta(t)) = C_{A0}(t)(1 + aE(t)), \qquad (3)$$

where $C_{A0}(t)$ is the concentration in maritime clean air and a is a factor relating emission rate $E(t)$ and relative local excess $\delta(t)$ of the trace gas. If the relative local excess for a certain time t_0 is known, for example through measurement of local air concentration or surface water in solubility equilibrium with the atmosphere, $\delta(t)$ can be expressed as

$$\delta(t) = aE(t) = \frac{\delta(t_0)}{E(t_0)} E(t). \qquad (4)$$

Measurement of SF_6 and CFC-113 concentrations in air and surface water at the study site suggested a

relative excess of 30% for SF_6 in 1995 and of 5% for CFC-113 in 1990, and the input functions were corrected according to Eqs. (3) and 4).

2.3. Excess air in water

Supersaturation of air in water may occur due to dissolution of air bubbles, resulting in 'excess air' (Mazor, 1972; Herzberg and Mazor, 1979; Heaton and Vogel, 1981; Rudolph et al., 1983; Andrews and Hussain, 1988; Stute, 1989). Air bubbles are trapped when the water table is rising and are completely dissolved by the rising hydrostatic pressure (Stute, 1989). Since SF_6 and CFC-113 are components of the entrapped air, excess air will lead to enhanced concentrations of these tracers in groundwater. In the presence of excess air, measured dissolved concentrations of the atmospheric trace gases have to be corrected (see below). Otherwise the inferred groundwater ages would be too young. Because ^3H is part of the water molecule itself, it is not affected by excess air. As mentioned above, ^{85}Kr values are also not affected, because they are normalised to the total amount of Kr in the water sample (specific activity; Cook and Solomon, 1997).

To quantify excess air in groundwater the Ne isotope ^{20}Ne was used, because atmospheric Ne concentrations are constant over time and the atmosphere is the only Ne source for shallow groundwater. The equilibrium concentration of ^{20}Ne in a groundwater sample can be calculated using the known solubility of ^{20}Ne, (the Bunsen coefficient of ^{20}Ne is $10\ cm^3$ STP kg^{-1} for freshwater at 10°C; Weiss, 1971), the constant ^{20}Ne concentration in the atmosphere (16.45 ppm; Ozima and Podosek, 1983) and the groundwater temperature. The amount of excess air can then be determined from the difference between calculated equilibrium concentration and actually observed ^{20}Ne concentration.

2.4. Sampling and measurement techniques

Four observation points and two drinking water supply wells were used for determination of hydraulic heads and for groundwater sampling (Fig. 2). Observation points are fully screened wells with a diameter of 150 mm except for GWM AB which has an diameter of 125 mm. At the supply wells groundwater was sampled by using two existing submerged pumps. At the observation points a portable submersible pump (Grundfoss MP1) was used. Prior to sampling, the borehole and all fittings were flushed with groundwater until at least three times the borehole volume was extracted. Oxygen concentration, water temperature, electrical conductivity and pH were monitored until measured values were stable. Finally, the groundwater samples for tracer measurements were collected as described below.

Most ^3H samples were collected and analysed by the National Research Center for Environment and Health (GSF) at Neuherberg, Germany (Graf, 1995). Additional groundwater samples for ^3H measurements were taken by the Institute of Environmental Physics, Heidelberg and measured by low-level counting with a standard deviation of ±5–10% and a detection limit of 1–2 TU (G. Bader, pers. communication).

All ^{85}Kr samples were collected by and measured at GSF (Graf, 1995). 200 l of groundwater were taken in stainless steel or polyethylene tanks. Extraction of dissolved krypton was performed by stripping the water with helium and subsequent adsorption of Kr in a cooled charcoal trap. Krypton was enriched in the gas mixture by adsorption and repeated desorption caused by slowly increasing the temperature of the charcoal trap. Finally, krypton was separated by gas chromatography with a charcoal column held at approximately 45°C. The amount of krypton in the gas mixture was determined with a thermal conductivity detector whereas the amount of ^{85}Kr was measured with a proportional counter. Detection limit is about 25 mBq $(cm^3$ STP $Kr)^{-1}$. The sampling and analytical methods for measurements of ^{85}Kr are described in detail by Held et al. (1992).

Samples for CFC measurement were collected in 500 ml glass bottles preventing contact of the sample water with atmospheric air. The sample bottles were filled submerged in a container filled with groundwater. The bottles were closed and transported submerged in sample water (Oster et al., 1996). Prior to sampling, the bottles as well as all fittings were flushed with 10 l of sample water (i.e. 20 times the sample volume). Measurements were carried out as soon as possible after sampling, usually within 24 h. After extracting the CFCs from 20 ml of the water sample by gas stripping with carrier gas, the concentrations of CFCs were determined by gas

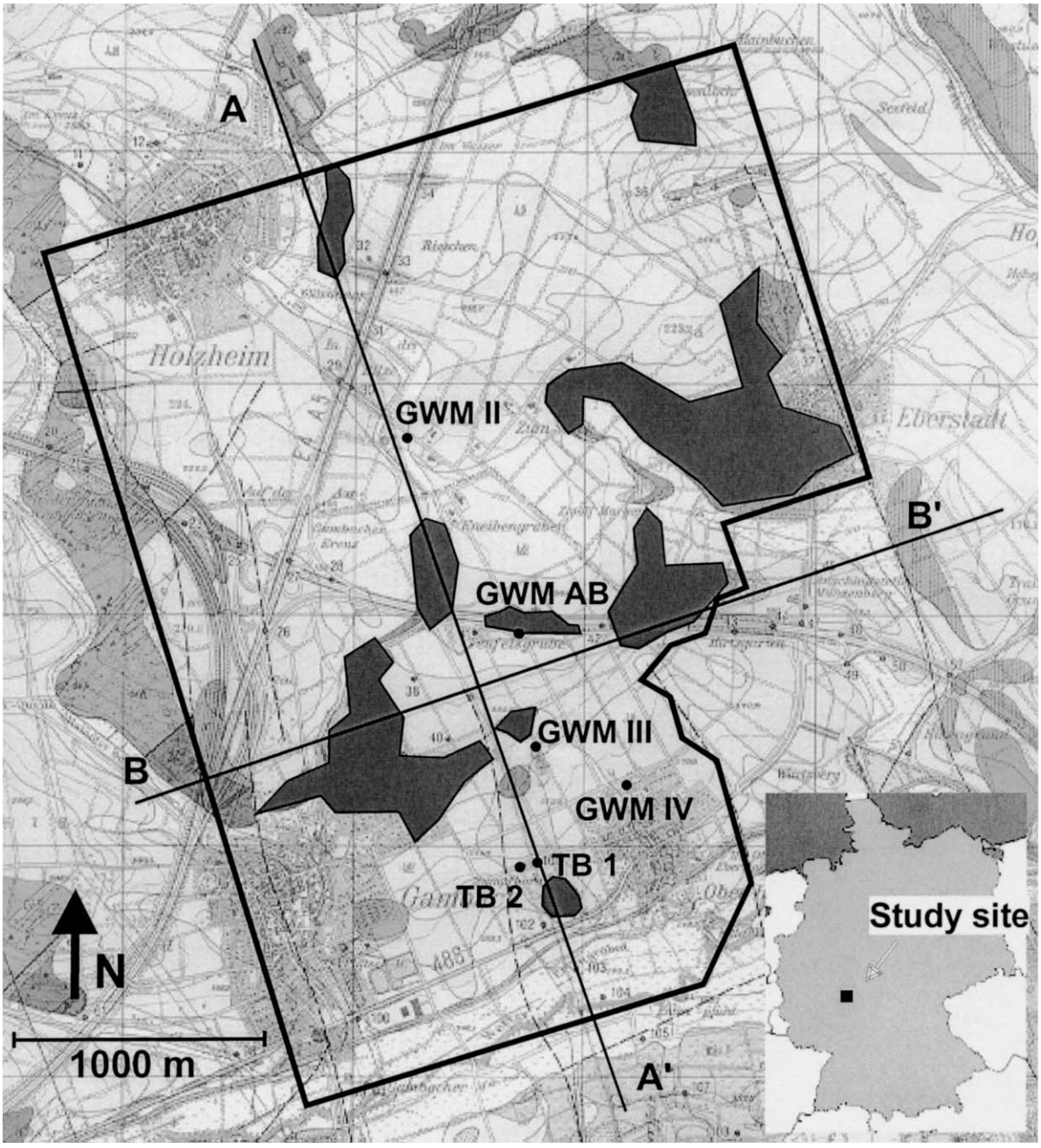

Fig. 2. Map of Gambach field site with delineation of model area, cross-sections AA′ and BB′, and location of sampling sites. Areas of basalt outcrop are shaded.

chromatography, using an electron capture detector (ECD) and a ultrapure mixture of argon (95%) and methane (5%) as carrier gas. After pre-concentration (−25°C) and desorption (90°C) in an adsorption trap, the CFCs were separated in two Porasil C columns (15 cm and 3 m of length, respectively). Calibration was performed by using a gravimetric standard from the National Oceanic and Atmospheric Administration (NOAA; Montzka et al. (1992)). Detection limit is about 0.1 fmol. The system and measurement procedures are described in more detail by Oster et al. (1996).

In order to quantify the total sampling and measurement error, 20 replicate samples were analysed for CFC-113, with concentrations ranging from 60 to 2850 fmol l^{-1}. Mean concentrations and standard deviations were calculated for each sample. Reproducibility, expressed as the mean of all relative standard deviations of the replicate samples, is ±5.2%.

For sampling of SF_6, 550 ml glass bottles with PVC fittings were used, similar to that used by Wanninkhof et al. (1991). The bottles were flushed with approximately 6 l of sample water and filled preventing contact of the water with the atmosphere. Preliminary studies have shown that this type of bottle is air tight and that samples can be stored for several weeks. SF_6 is extracted from the groundwater sample by injecting a headspace of approximately 50 ml of nitrogen into the sample bottle. Because of the low solubility of SF_6, 99% of SF_6 in the sample water enters the headspace when shaking the bottle for 20 min. The headspace is then injected into the sample loop of the gas chromatograph.

SF_6 was measured using the gas chromatographic system described in detail by Maiss et al. (1996). Ultrapure nitrogen was used as carrier gas and SF_6 was separated from other components in columns filled with molecular sieve (5 Å). Column and ECD temperature were held at 65 and 330°C, respectively. A purge-and-trap technique was used to pre-concentrate SF_6 (temperatures of −77 and 100°C for trapping and releasing, respectively). Detection limit is 0.015 fmol (Maiss et al., 1996). Calibration was performed using a gravimetrically produced standard containing a mixture of ultrapure nitrogen and SF_6 (Maiss, 1992). Sampling and measurement techniques are described in more detail by Fulda and Kinzelbach (1998).

Mean values and standard deviations were determined for 70 replicate samples, with concentrations ranging from 0.1 to 50 fmol l^{-1}. Reproducibility, expressed as the average of the relative standard deviations of all replicates, is ±3.1%.

Samples for Ne were taken in 40 ml copper tubes. The tubes were flushed with approximately 10 l of sample water. Ne was vacuum extracted and measurement of Ne isotopes was performed using quadrupole mass spectrometry. Detection limit is about 2×10^{-10} cm^3 STP (Rupp, 1993). Replicate groundwater samples show a reproducibility of Ne measurements of about ±2%.

3. Site characterisation

The field site is located near the village of Gambach in the state of Hessen, approximately 50 km north of Frankfurt/Main, Germany (Figs. 2 and 3). It belongs to the agricultural area of the Wetterau region, a geological depression surrounded by the Vogelsberg and Taunus Mountains. The aquifer consists of basalt rocks of Miocene age and is underlain by silty Miocene and Oligocene sediments (Rockenberger Schichten). It is mainly overlain by loess deposits of variable thicknesses stretching a range between 3.5 m and a maximum of 15 m. Aquifer thickness varies from 2 to 25 m with a mean value of 20 m (Fig. 3). The basalt rock of the aquifer is fractured and highly permeable. Transmissivity, as determined by several pumping tests, varies from 0.8 m^2 d^{-1} at GWM II to 280 m^2 d^{-1} at TB 1 and TB 2. The underlying silty Miocene and Oligocene sediments are much less permeable than the fractured basalt rock of the aquifer and can be considered as aquitards. The aquifer is drained by the Wetter river, with flow mainly from the north to the south. The groundwater flow system has been described in detail by Vassolo (1995) and Vassolo et al. (1998), and more information on the site can as well be found in Zoellmann et al. (2001).

4. Results

Four observation wells and two water supply wells were used as sampling sites for this study. All were sampled for ^3H and the trace gases CFC-11, CFC-12, CFC-113, ^{20}Ne and SF_6. ^{85}Kr samples were taken at

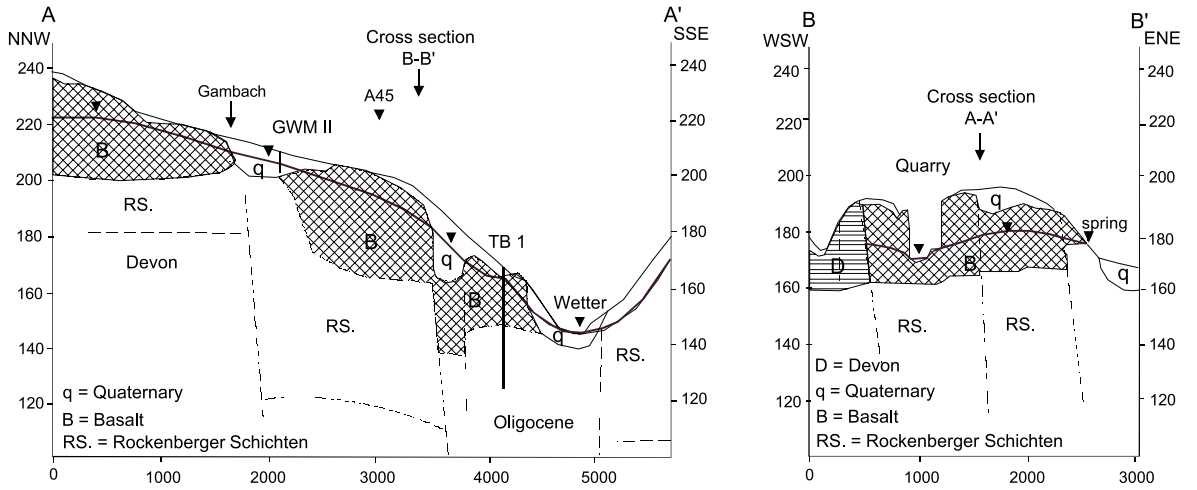

Fig. 3. Cross-sections of the Gambach field site along AA′ and BB′. For location of cross-sections see Fig. 2.

four of the six sampling sites. Measured values, except for CFC-11 and CFC-12, are listed in Tables 1–3 and are graphically shown in Figs. 5 and 6. In all wells CFC-11 and CFC-12 concentrations were up to 10 times higher than solubility equilibrium with ambient air. This large discrepancy cannot be explained by excess air. Instead a contamination of the groundwater with these two CFCs has to be assumed. They could not be interpreted with regard to groundwater residence times. Similar enhanced concentrations of chlorofluorocarbons excluding their use as age dating tracers were reported for a number of other field studies (e.g. Thompson and Hayes, 1979; Busenberg and Plummer, 1992; Jackson et al., 1992).

^{3}H concentrations show large variations from 4.5 TU at well GWM III to 59 TU at well GWM IV (Table 1). Concentrations at wells GWM AB, TB 1 and TB 2 show a slight decrease with time whereas concentrations at wells GWM II and GWM III are nearly constant. ^{3}H concentrations at well GWM IV are very high and variable in time (32–59 TU).

Specific activities of ^{85}Kr vary from 21 dpm (cm^3 STP)$^{-1}$ at well GWM III to 52 dpm (cm^3 STP)$^{-1}$ at TB 1 (Table 2). The measurement error is relatively large (cf. Table 2). The specific ^{85}Kr activity measured at well TB 1 is higher than ^{85}Kr activities observed in the other wells. This result was surprising since well TB 1 is located downstream of the other wells (Figs. 2 and 4) and should therefore receive water that has already passed the other wells. The expected longer residence time should result in lower specific activities in TB 1 as compared to the upstream wells. The high value cannot be explained by a very young water component in TB 1, as this should also lead to high concentrations of the other tracers in TB1 that is not observed. A contamination of the ^{85}Kr sample with atmospheric air could have caused this high value.

Observed concentrations of CFC-113 cover the range from 318 fmol l^{-1} at GWM III to 538 fmol l^{-1} at GWM AB (Table 3). The lowest CFC-113 concentrations were found at GWM III. The values at TB 1, TB 2 and GWM AB are strongly variable in time.

Dissolved oxygen concentrations between 7 and 10 mg l^{-1} have been found at all sampling points except for well GWM II (1.4 mg l^{-1}). These values confirm that the aquifer is generally oxic and therefore degradation of CFC-113 is not expected (Cook and Solomon, 1997).

Measured concentrations of SF_6 vary from 1.08 fmol l^{-1} at TB 2 to 6.25 fmol l^{-1} at GWM IV (Table 3). Wells TB 1, TB 2 and GWM IV show SF_6 concentrations clearly above the solubility equilibrium. The SF_6 concentration of groundwater in solubility equilibrium with 1995 atmospheric air is 1.92 fmol l^{-1} (local SF_6-excess: 30%, groundwater temperature: 10°C). Maximum observed concentrations at wells TB 1 and TB 2 were 2.31 and 2.38 fmol l^{-1}, respectively, and were reached in 1994 and 1995. The maximum concentration at GWM IV was 6.25 fmol l^{-1} in

Table 1
^{3}H measurements at the Gambach field site. Values denoted with * were measured at IUP, Heidelberg. All other values at GSF, Neuherberg

Sampling date	TB 1 (TU)	TB 2 (TU)	GWM AB (TU)	GWM II (TU)	GWM III (TU)	GWM IV (TU)
20/03/91	24.2	25.5				
19/11/91	34.3	24.2				
28/04/92	24.7	26.0				
16/03/93	24.5	24.8	29.1	18.8	6.5	33.9
30/03/93	23.7	23.3		17.7	4.5	46.6
14/04/93	21.7	21.6		15.7	5.5	43.6
28/04/93	22.8	21.0	27.2	17.7	7.2	46.4
05/05/93						
11/05/93	23.5	24.9	30.0	19.9	4.8	49.7
23/06/93	27.7	24.7	29.2	17.5	5.6	59.2
13/12/93						48.0
19/01/94	23.7				7.6	
20/01/94				18.9		
24/04/94						50.3*
27/04/94			22.8*	17.6*	10.8*	54.2*
05/11/94	22.9*	20.9*	25.6*			48.2*
24/05/95	20.9*	19.9*	21.5*			32.6*
29/08/95			22.6*	19.3*		
25/09/95					8.8*	
04/12/95	20.4*	20.9*	23.2*			41*

1994. The increased concentrations cannot be explained by excess air and are possibly caused by a local SF_6 contamination event which was located downstream (south) of GWM III (which was not affected by the enhanced concentrations) and near GWM IV. The assumed spill time is 1992 or 1993.

Concentrations of the noble gas isotope ^{20}Ne were determined for all wells and most of the sampling dates (Table 2). Values reach from 1.95×10^{-7} cm^3 STP g^{-1} at TB 1 to 2.4×10^{-7} cm^3 STP g^{-1} at GWM II. Values are nearly constant with time for each of the sampling points.

5. Discussion

5.1. Excess air

As already discussed before, groundwater concentrations of ^{3}H and ^{85}Kr are not affected by excess air. However, total groundwater concentrations of CFC-113 and especially of SF_6 may become enhanced by excess air. For a chemically inert gas of species i the concentration in water C_{Wi} is given by

$$C_{Wi} = \alpha_i C_{Ai} + \Delta C_{Ai} = (\alpha_i + \Delta) C_{Ai}, \quad (5)$$

where $\alpha_i = \alpha_i(T)$ denotes the solubility of gas i for freshwater, T the recharge temperature, Δ the amount of excess air relative to the equilibrium concentration of air in groundwater and C_{Ai} is the atmospheric concentration of gas i. The first term on the right hand side represents the concentration of gas i in a water sample which results from solubility equilibrium with the ambient soil air at the groundwater table at temperature T. The second term represents the effect of excess air on dissolved concentration of a gas i in groundwater. Excess air increases the concentration of gas i in groundwater by ΔC_{Ai}. The total concentration of gas i in a water sample is increased relative to equilibrium solubility by a factor

Table 2
^{85}Kr measurements at the Gambach field site. Error is one standard deviation

Well name	Sampling date	^{85}Kr dpm cm^{-3}	Error dpm cm^{-3}
TB 1	14/12/93	51	5
GWM II	20/01/94	33	4
GWM III	19/01/94	24.5	6
GWM IV	13/12/93	42	7

Table 3
CFC-113, SF_6 and ^{20}Ne measurements from the Gambach field site. Included are excess air and the concentrations of CFC-113 and SF_6 corrected for excess air, $CFC\text{-}113_{corr}$ and SF_{6corr}

Sampling well	Sampling date	CFC-113 (fmol l^{-1})	SF_6 (fmol $l^{-1)}$	Temperature (°C)	^{20}Ne (Nml gH_2O^{-1})	Excess air (cm^3 kgH_2O^{-1})	$CFC\text{-}113_{corr}$ (fmol l^{-1})	$SF_{6\ corr}$ (fmol l^{-1})
GWM AB	29/04/93		1.73					1.53
GWM AB	07/07/94	520.3	1.62	11.3			514.9	1.40
GWM AB	07/07/94		1.65					1.43
GWM AB	18/11/94	414.7	1.68	10.8	2.096×10^{-7}	1.92	408.3	1.42
GWM AB	28/05/95	457.0	1.61	11.6	2.016×10^{-7}	1.49	451.9	1.39
GWM AB	30/08/95	494.7	1.69	11.7	2.019×10^{-7}	1.50	489.6	1.47
GWM AB	30/08/95	455.4					449.9	
GWM AB	07/12/95	538.3	1.78	11.0			532.7	1.54
GWM IV	30/04/93		1.73					1.33
GWM IV	07/07/94	443.4	6.25	11.7			432.0	5.80
GWM IV	07/07/94	437.4	5.40				426.0	4.95
GWM IV	18/11/94	481.7	3.20	11.2	2.326×10^{-7}	3.30	470.5	2.76
GWM IV	28/05/95	454.5	1.98	11.5	2.341×10^{-7}	3.41	442.4	1.48
GWM IV	07/12/95	489.5	2.90	11.3	2.336×10^{-7}	3.36	447.7	2.40
GWM III	27/04/94			10.9	2.242×10^{-7}	2.78		
GWM III	07/07/94	318.4	1.14	10.9			312.1	0.89
GWM III	07/07/94	368.3	1.14				362.0	0.89
GWM III	28/09/95	318.6	1.20	10.8	2.336×10^{-7}	3.29	311.3	0.91
TB 1	14/07/92		1.30					1.22
TB 1	05/08/92		1.40					1.32
TB 1	30/04/93		1.93					1.84
TB 1	18/11/94	376.1	2.31	10.6	1.951×10^{-7}	0.95	373.5	2.21
TB 1	18/11/94	340.3	2.28		1.930×10^{-7}	0.84	337.9	2.18
TB 1	28/05/95	475.9	2.22	10.9	1.961×10^{-7}	1.07	472.8	2.10
TB 1	28/05/95	383.2	2.16				380.1	2.03
TB 1	07/12/95	484.0	1.89	10.5			481.3	1.78
TB 2	14/07/92		1.40					1.30
TB 2	05/08/92		1.50					1.40
TB 2	30/04/93		1.08					0.97
TB 2	18/11/94	399.0	2.25	10.7	1.952×10^{-7}	0.97	396.1	2.14
TB 2	18/11/94				1.983×10^{-7}	1.16		2.13
TB 2	28/05/95	408.8	2.38	10.9	1.987×10^{-7}	1.21	405.3	2.24
TB 2	07/12/95	524.6	2.16	10.5	2.002×10^{-7}	1.32	520.8	2.01
GWM II	27/04/94			10.7	2.422×10^{-7}	3.75		
GWM II	30/08/95	399.1	1.66	10.5	2.390×10^{-7}	3.66	387.8	1.19

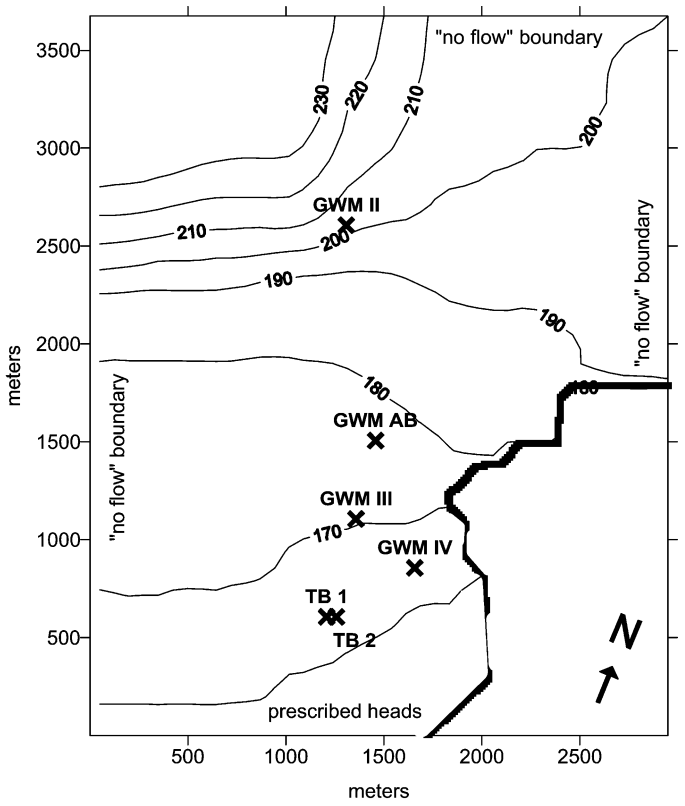

Fig. 4. Model area with boundaries, simulated piezometric heads (June 1994), location of water supply wells (TB 1, TB 2) and observation wells (GWM II, GWM III, GWM IV, GWM AB).

F_{ea}:

$$F_{ea} = \frac{C_{Wi}}{\alpha_i C_{Ai}} = 1 + \frac{\Delta}{\alpha_i}. \quad (6)$$

Therefore, the lower the solubility α_i of a gas i, the more pronounced is the relative effect of excess air on the total gas concentration.

Measured Ne data and groundwater temperatures were used to calculate the excess air for each well and sampling date separately (see Table 3). Because groundwater temperatures in all wells and at all times agree within ± 1°C, the observed temperature was assumed to correspond to the temperature in the recharge area, and was used to calculate the excess air. A groundwater temperature variation of ± 1°C would lead to a variation of the calculated excess air of approximately $\pm 0.1\ cm^3\ kg^{-1}$. Excess air values vary from $0.84\ cm^3\ kg^{-1}$ at TB 1 to $3.75\ cm^3\ kg^{-1}$ at GWM II, with a mean of $2.1\ cm^3\ kg^{-1}$. These values are within the range reported for other sites in Germany (Rudolph et al., 1983). The amount of excess air differs between individual wells, but varies only little in time for the individual wells (within 3%).

Solubility of CFC-113 is $148\ cm^3\ kg^{-1}$ at 10°C which is much larger than the maximum value of excess air measured at this field site of $3.75\ cm^3\ kg^{-1}$. The solubility of SF_6 is only $10\ cm^3\ kg^{-1}$ which is of the same order of magnitude as excess air. Eq. (6) shows that up to 30% of the measured SF_6 in our groundwater samples may originate from excess air. Therefore, the measured SF_6-concentration must be corrected for excess air.

Whereas atmospheric ^{20}Ne concentrations are constant in time, atmospheric concentrations of CFC-113 and SF_6 show a strong increase over the past decades (Fig. 1). Entrapment of excess air will presumably occur during seasonal groundwater table fluctuations. Therefore, a water sample may contain

excess air from more than one recharge event. Accordingly the atmospheric concentrations of the tracer gases that are contained in excess air may represent a mixture of concentrations over a certain time interval. An ideal mixing model (Kaufman and Libby, 1954) and an iterative predictor-corrector scheme were used to estimate the effective mean atmospheric concentrations of the tracer gases for excess air correction of the water samples. The original tracer gas concentration in the water sample c_0 is corrected by using the excess air value Δ of the well determined from Ne concentrations and an atmospheric tracer gas concentration c_{A1}, corresponding to an arbitrarily chosen model age τ_1. The corrected tracer gas concentration in the water sample c_1 is then used to determine the related new model age τ_2. Based on the new model age τ_2 a new atmospheric trace gas concentration c_{A2} is calculated. Correcting c_0 with Δc_{A2} yields a new concentration c_2 of the tracer in the water sample. This iterative correction is repeated until the difference between two subsequent corrected concentrations c_{n-1} and c_n is less than a given threshold value

$$c_n = c_0 - \Delta c_{An}(\tau_n), \tag{7}$$

$$\tau_n = \mathrm{MA}(c_{n-1}),$$

$$\frac{|c_n - c_{n-1}|}{c_{n-1}} < 10^{-3},$$

where $\mathrm{MA}(c_{n-1})$ denotes the model age determined from the tracer concentration c_{n-1} in the water sample. This correction scheme is not limited to the specific model assumption underlying the determination of the model age τ. In other cases a piston flow model or a general transfer function approach (Amin and Campana, 1996) may be used. In case of complex aquifer geometries or boundary conditions, the model age τ may be obtained by determining the transfer function from the numerical flow model.

If Ne data were available for the actual sampling date and sampling well, CFC-113 and SF_6 concentrations were corrected using these data (see Table 3). Concentrations for other sampling dates were corrected by the average excess air value for the corresponding well. The error introduced by averaging is small since excess air values were nearly constant in time for all wells of the study site. Mean excess air correction of CFC-113 reduced the measured concentrations by only 1.5%, the maximum correction is 2.8% at GWM II. This correction is less than the measured reproducibility for CFC-113 and can therefore be neglected. However, mean excess air correction for SF_6 reduced the measured SF_6 concentrations of the water samples by 12%. At GWM II, where highest values for excess air have been measured, the correction amounts to 28%. Whereas excess air correction is not important for CFC-113, it is essential for SF_6, making determination of excess air a necessity for groundwater age dating using SF_6.

5.2. Modelling

The regional flow and transport model of the study site from Vassolo et al. (1998) and Zoellmann et al. (2001) was used to simulate ^{85}Kr, ^{3}H, SF_6 and CFC-113 transport in the subsurface (see Fig. 4). A confined and isotropic aquifer was assumed (Vassolo et al., 1998). A two-dimensional approach was chosen using the USGS finite difference model MODFLOW (McDonald and Harbaugh, 1988). Transport modelling was performed using the MT3D code (Zheng, 1990) on a monthly basis. The northern model boundary is given by a flow divide. The impervious western and eastern boundaries of the model follow the courses of geological faults. To the south a prescribed head boundary is formed by the river Wetter that receives most of the water recharged in the model area. Groundwater flow is mainly directed from north to south. Mean groundwater recharge amounts to 100 mm a^{-1}. The major part of the aquifer is covered by loess deposits of variable thickness. Since the loess deposits with maximum thicknesses of up to 15 m (MLU, 1980) are characterised by a very high specific water retention capacity, long residence times of the water-bound tracer ^{3}H in the unsaturated zone can be expected.

Explicit consideration of the unsaturated zone and the spatial variability of its thickness is essential for modelling of ^{3}H concentrations at this field site as total ^{3}H residence time and its spatial distribution in the system are strongly influenced by the transport through the unsaturated zone. In this study a simple model is used to account for the spatially varying residence times of ^{3}H in the unsaturated zone (Zoellmann et al., 2001). Transport of ^{3}H through the unsaturated zone is assumed to be piston-flow like, i.e. the amount of

water added at the top of the unsaturated zone by infiltration in a given time increment is equal to the amount of water recharged to the aquifer. The ^{3}H concentrations are corrected for radioactive decay during transport through the unsaturated zone. Calculations show that the mean residence time of ^{3}H in the loess deposits may be considerably larger than in the basalt rock aquifer itself. Residence times of ^{3}H in the unsaturated zone calculated with the piston-flow type model can be as large as 30 years in areas of thick loess cover (Zoellmann et al., 2001) while mean residence time in the saturated aquifer varies between 4 and 6 years, as determined from modelling of the gaseous tracers (see below). It should be noted that the concentrations of the gaseous tracers at the water table are only slightly affected by the loess deposits, as molecular diffusion in soil air allows for a rather rapid transport of atmospheric gases through the unsaturated zone. Calculations show that the loess cover may result in a maximum delay of 1 year for the atmospheric gaseous tracers (Cook and Solomon, 1995).

An important parameter for tracer transport in the aquifer is the effective porosity n_e of the medium. It comprises that fraction of the porous medium that is water-filled and contributes to species transport. Its value affects both the tracer residence time and the depth averaged tracer concentrations. A certain amount of tracer reaching the groundwater surface at a certain time will overlie a body of older water with a different mean concentration. The relative contribution of a given amount of freshly recharged tracer to the depth averaged concentration will be larger for low values of n_e, as 'dilution' of the recharging water is small in this case. Depth averaged concentrations were obtained from the fully screened observation and pumping wells at the study site and were the basis for calibration of the transport model. The effective porosity was the only parameter used to calibrate the transport model of the saturated zone by means of the measured tracer concentrations, and is constant within the whole model area.

Using the known input functions for ^{3}H and ^{85}Kr (Fig. 1), the best match between observed and modelled concentrations of these tracers is obtained using an effective porosity of $n_e = 0.07$. Simulated concentrations of ^{85}Kr match the observed concentrations at wells GWM II, GWM III and GWM IV (Figs. 5a and 6a). However, the database is sparse as there is only one ^{85}Kr measurement for each site. The exceptionally large ^{85}Kr concentration measured at well TB 1 cannot be reproduced by the model. As mentioned before this is presumably due to a sample contamination because a much smaller ^{85}Kr concentration is anticipated for this well from flow pattern and concentration of the other tracers.

Modelled concentrations of ^{3}H using an effective porosity of $n_e = 0.07$ (Figs. 5b and 6b) agree well with observed ^{3}H at TB 1, TB 2 and GWM II. At GWM AB agreement of calculated and measured ^{3}H concentrations is satisfying although simulated concentrations are somewhat too low in spring 1993. At GWM IV, the trend of the observed peak-like ^{3}H concentration course can be reproduced with the model. Also, the maximum concentration of about 50 TU was confirmed by the calculations. However, the modelled ^{3}H peak at GWM IV arrives approximately 1 year too early. This is probably caused by a slight underestimation of the unsaturated zone thickness at this location. The enhanced concentrations in GWM IV are caused by relatively old, ^{3}H-rich water recharged in an area with very long residence times in the loess deposits reaching the sampling location between 1993 and 1996. An even better correspondence between observed and simulated ^{3}H data at GWM IV and GWM AB would have been achieved by decreasing the effective porosity n_e to about 0.03, as this would lead to larger (less diluted) depth averaged concentrations. However, a lower effective porosity would in turn lead to high simulated ^{85}Kr concentrations. At GWM III a large discrepancy between measured and simulated ^{3}H values is observed. The ^{3}H values are exceptionally low and cannot be explained by the model. This may be a limitation of the two-dimensional modelling approach, as e.g. interaction with the underlying aquifer may be erroneously neglected in this case.

For simulation of SF_6 transport, the atmospheric SF_6 input function was modified in the way described in Section 2.1 (Eqs. (3) and (4)) to account for the continental SF_6 excess of 30%. The enhanced SF_6 concentrations in GWM IV, TB 1 and TB 2 were not considered during model calibration. Best model results for SF_6 are obtained using an effective porosity of 0.07 (Figs. 5d and 6d). This corresponds well with the effective porosity obtained from ^{85}Kr modelling.

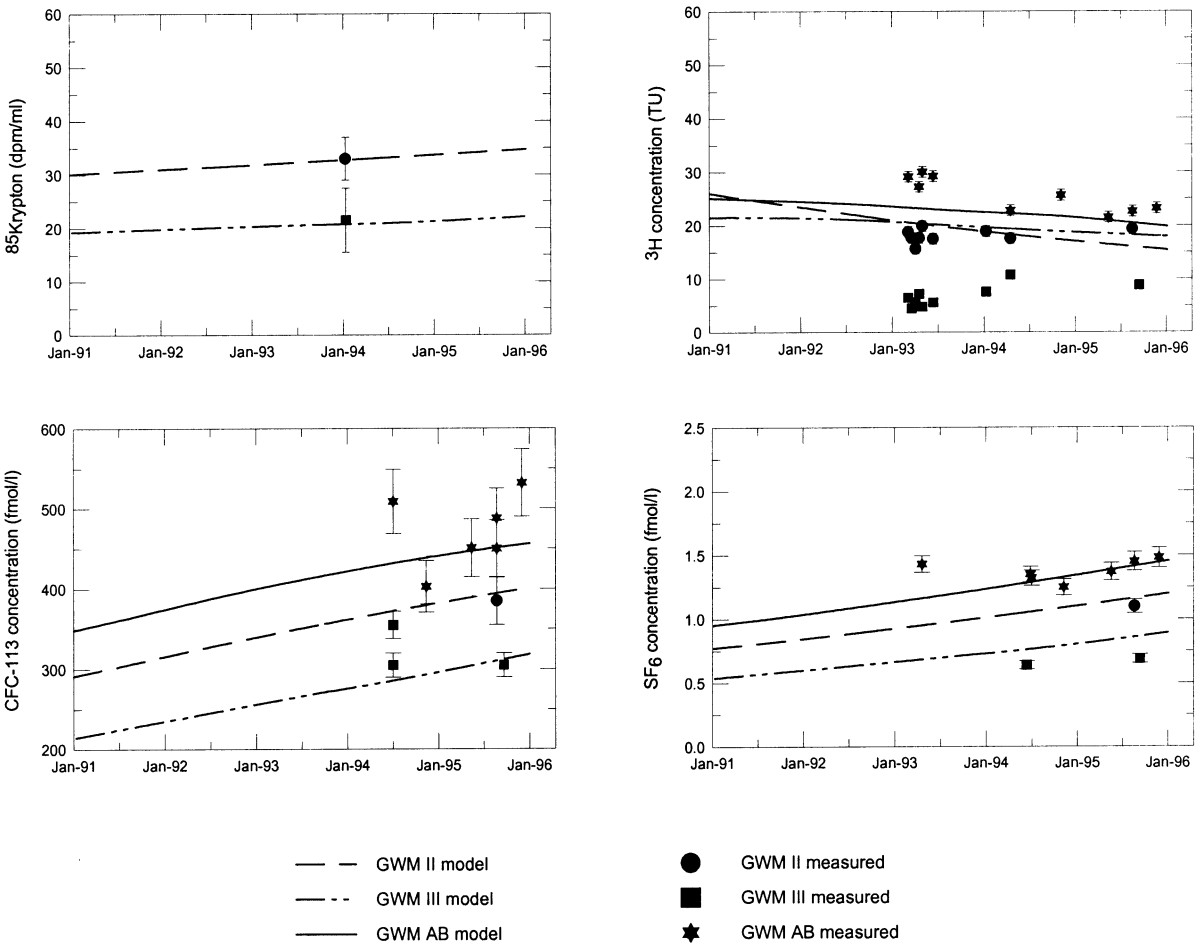

Fig. 5. Measured and simulated concentrations of ^{85}Kr (a), ^{3}H (b), CFC-113 (c) (corrected for excess air) and SF_6 (d) (corrected for excess air) at Gambach field site for GWM II, GWM III and GWM AB. Transport simulation was performed with an effective porosity $n_e = 0.07$ for all tracers, input function for SF_6 and CFC-113 which are corrected for continental excess, a retardation factor of $R = 1.5$ for CFC-113 and explicit consideration of advective ^{3}H transport through the unsaturated zone.

Simulated and measured concentrations of SF_6 agree within reproducibility at wells GWM AB, GWM II and GWM III (Fig. 5d) except for the first measurement in GWM AB in 1993. Fig. 6d suggests that water with enhanced SF_6 concentrations reached the wells TB 1, TB 2 and GWM IV between 1992 and 1994. In 1995 concentrations seem to decrease again in wells TB 1 and TB 2 while no clear trend can be observed for GWM IV. The simulated results for SF_6 at the observation wells GWM II, GWM III and GWM AB confirm the effective porosity of 0.07 already obtained from ^{85}Kr and ^{3}H modelling.

For modelling of CFC-113 concentrations a slight atmospheric excess of 5% in 1990 was assumed and the input function modified according to Eqs. (3) and (4). Best results were achieved using an effective porosity n_e of 0.13. However, this value is not very likely for a fractured basalt aquifer and it conflicts with the results from ^{85}Kr, ^{3}H and SF_6 modelling which suggest an effective porosity of 0.07. Modelling exercises showed that it was not possible to reproduce measured SF_6, ^{85}Kr and especially ^{3}H data using a porosity value of 0.13. Using this large porosity the simulated concentrations of these tracers reached only about half of the observed values.

As the simulated CFC-113 concentrations in the

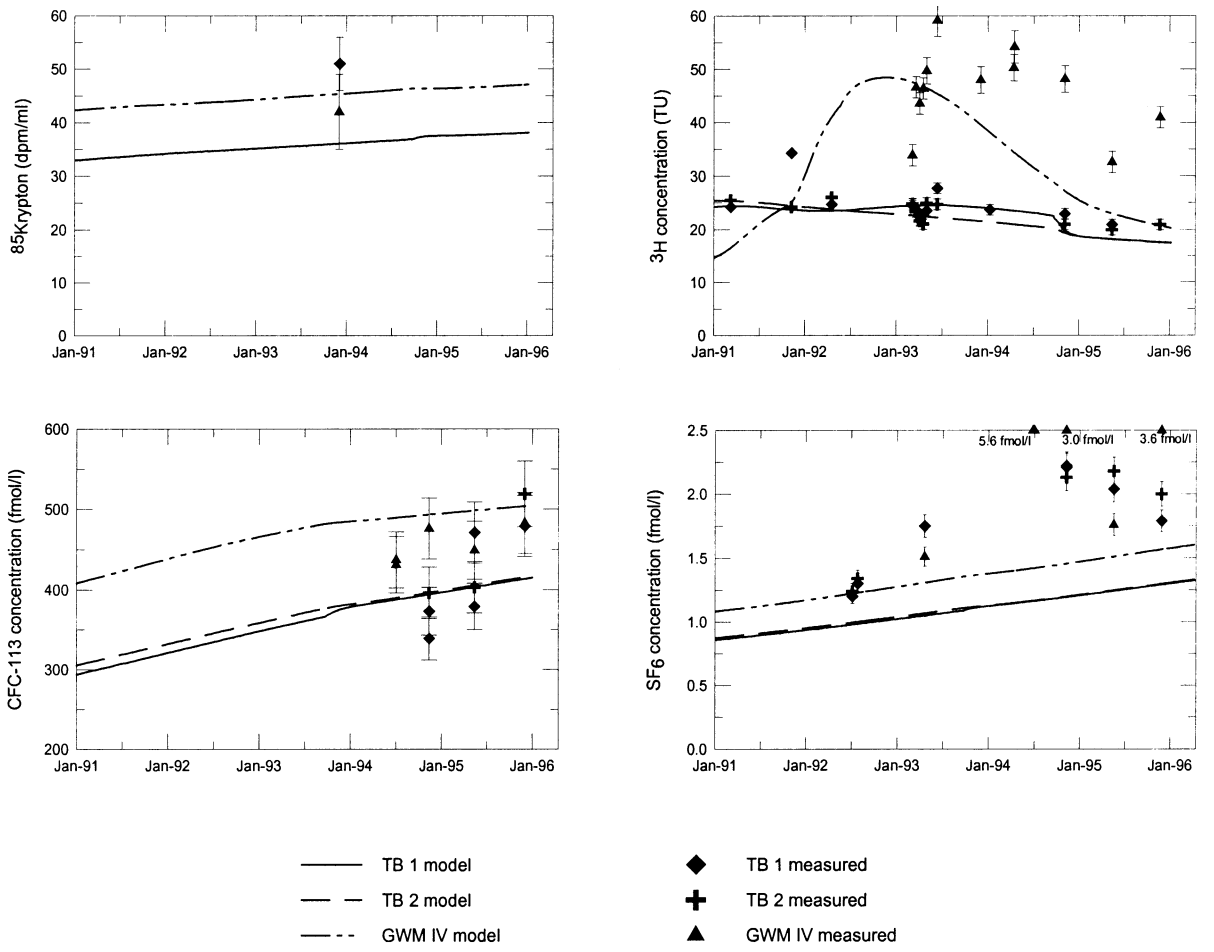

Fig. 6. Measured and simulated concentrations of ^{85}Kr (a), ^{3}H (b), CFC-113 (c) (corrected for excess air) and SF_6 (d) (corrected for excess air) at Gambach field site for TB 1, TB 2 and GWM IV. Transport simulation was performed with an effective porosity $n_e = 0.07$ for all tracers, input function for SF_6 and CFC-113 which are corrected for continental excess, a retardation factor of $R = 1.5$ for CFC-113 and explicit consideration of advective ^{3}H transport through the unsaturated zone. Note the large variance in ^{3}H concentrations caused by the storage effect of the unsaturated zone.

aquifer were too large when using an effective porosity of 0.07, we also considered the effect of a reduced atmospheric excess for CFC-113. The continental excess of 5% was already a moderate value, but even if no continental excess at all was assumed (which is not realistic), simulated concentrations are still appreciably higher than the measured values. A higher continental excess for CFC-113 would even further increase the model concentrations and could thus not explain the CFC-113 values. Also, all possible atmospheric contamination of CFC-113 would lead to higher atmospheric concentrations and thus to higher concentration values in the aquifer, which would conflict with the measured values of CFC-113.

Longer residence time of CFC-113 in the unsaturated zone could lead to a reduced input signal at the aquifer top and thus to lower concentrations in groundwater. To reproduce the observed CFC-113 concentrations in groundwater with an effective porosity of 0.07, a mean residence time in the unsaturated zone of 2.5 years is needed, which corresponds to a mean thickness of the unsaturated zone of about 20 m (using an effective diffusion coefficient in the unsaturated zone of $5 \times 10^{-6}\,m^2\,s^{-1}$, (Gölthenboth,

1997). However, maximum thickness of the unsaturated zone in the model area is about 15 m and mean thickness is about 8 m which corresponds to a mean residence time of less than 1 year. In addition, a thicker unsaturated zone would also affect the results for the other gaseous tracers, which have similar diffusion coefficients, and leads to reduced concentrations in groundwater. Therefore an increased residence time of CFC-113 in the unsaturated zone is not likely the explanation for the relatively low observed CFC-113 concentrations.

Since CFC-113 transport in groundwater may be affected by adsorption to the aquifer material (see Section 2.1), a linear, instantaneous and reversible adsorption term was included in the modelling of CFC-113 transport. Using the effective porosity of 0.07, confirmed by modelling of the ^{85}Kr, SF_6 and ^{3}H, a retardation factor of $R = 1.5$ allowed for best correspondence between observed and simulated CFC-113 concentrations (Figs. 5c and 6c). Simulated concentrations are in agreement with measured concentrations except for well GWM IV, where simulated values are too high by about 10%. The strong variability of measured CFC-113 concentrations with time is also not reproduced by the model.

Continental excess and adsorption have an opposite effect on CFC-113 concentrations in groundwater. In general, a higher continental excess could be compensated by a larger retardation factor. Additional model runs using a higher continental excess in combination with larger retardation factors revealed that the discrepancies between observed and simulated concentrations at well GWM IV are further increased. The reason for this is that the water entering GWM IV had experienced a shorter mean travel path in the aquifer than the water at the other sampling points. Therefore, increased input concentrations caused by increased continental excess is not sufficiently compensated by a larger retardation factor in well GWM IV. These findings support the small continental excess of 5% and the retardation factor of $R = 1.5$ chosen for CFC-113.

Fig. 7 shows simulated concentrations of CFC-113 with $R = 1$ and 1.5 versus measured concentrations. With no retardation of CFC-113 and an effective porosity of 0.07, modelled concentrations are generally higher than the observed values. Using a

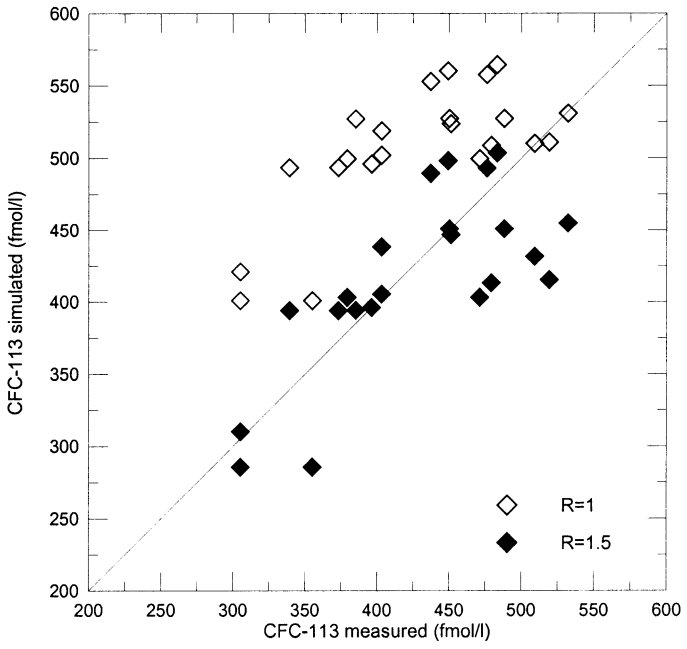

Fig. 7. Simulated concentrations of CFC-113 without retardation ($R = 1$, crosses) and with retardation ($R = 1.5$, diamonds) versus measured concentrations.

retardation factor of $R = 1.5$ improves the correspondence between measured and simulated data. Clearly, there is still appreciable scatter in Fig. 7. It is the result of the relatively low spatial and temporal resolution in our model, which was in turn dictated by our limited knowledge on spatial distribution of aquifer parameters and on the temporal distribution of the local tracer input functions. So we did not expect to exactly mach the concentrations in every single sampling point, but rather aimed at reproducing the general trends of the different tracers.

The retardation factor of $R = 1.5$ found here is in good agreement with other experimental and model findings, which give a range for CFC-113 from $R = 1.3–1.7$ (see Section 2.1 above; Ciccioli et al., 1980; Cook et al., 1995).

6. Conclusions

The findings described in the previous chapter suggest that a multi-tracer approach can significantly enhance the information gained when modelling a study site, because uncertainties are reduced by every additional tracer. Thus the approach of a multi-tracer study combined with numerical modelling seems promising. A multi-tracer study involving CFC-113 and one or more non-adsorbing tracers such as ^{3}H and ^{85}Kr may provide insight in effective adsorption processes for organic compounds on a regional scale. Sorption characteristics may be transferred from CFC-113 to comparable organic molecules, such as chlorinated aliphatic hydrocarbon contaminants, by first deriving the partition coefficient K_D for CFC-113 from the retardation factor according to Eq. (1). In the next step the K_D of any comparable organic compound could be estimated from the K_D for CFC-113 using physicochemical properties of the compounds, like for example solubilities in water or octanol–water partitioning coefficients. With this procedure one would arrive at a semi-quantitative estimate of the regional mean transport behaviour of certain organic contaminants. Estimates of the adsorption coefficients of these contaminants are not only important for the assessment of their residence times in the aquifer but also for the quantification of the total contaminant load of the aquifer, as even slight adsorption increases the total contaminant load considerably.

Using CFC-113 as a retardation tracer could be helpful for the prediction of organic contaminant transport or for the evaluation of possible hydraulic aquifer remediation measures. This is especially true as direct determination of regional mean adsorption characteristics through laboratory studies with aquifer material is generally not feasible due to the enormous amount of samples required to arrive at representative values. Moreover, results from laboratory studies cannot directly be applied to a certain field case but have to undergo a usually only vaguely known upscaling procedure. Although further investigations concerning the adsorptive behaviour of CFC-113 are necessary, i.e. further column studies or field evidence from other test sites, it becomes apparent that reactive tracers such as CFC-113 can significantly contribute to our understanding of regional transport processes in shallow aquifers.

Acknowledgements

We would like to thank M.E. Campana and two anonymous reviewers, who greatly improved the manuscript by their thoughtful reviews.

References

AFEAS, 1996. Production, sales and atmospheric release of fluorocarbons through 1994. Alternative Fluorocarbons Environmental Acceptability Study, Washington, USA.

Albritton, D.L., Derwent, R.G., Isaken, I.S.A., Lal, M., Wuebbles, D.J., 1994. Trace gas radiative forcing indices. In: Houghton, J.T., Meira Filho, L.G., Bruce, J., Lee, H., Callandar, B.A., Haites, E., Harris, N., Maskell, K. (Eds.). Climate Change 1994: Radiative Forcing of Climate Change and An Evaluation of the IPCC IS92 Emission Scenarios. University Press, Cambridge, pp. 204–231.

Amin, I.E., Campana, M.E., 1996. A general lumped parameter model for the interpretation of tracer data and transit time calculation in hydrologic systems. J. Hydrol. 179, 1–21.

Andrews, J.N., Hussain, N., 1988. Atmospheric and radiogenic gases in groundwaters from the Stripa granite. Geochim. Cosmochim. Acta 53, 1831–1841.

Ashton, J.T., Dawe, R.A., Miller, K.W., Smith, E.B., Stickings, B.J., 1968. The solubility of certain gaseous fluorine compounds in water. J. Chem. Soc., A, 1793–1796.

Bu, X., Warner, M.J., 1995. Solubility of chlorofluorocarbon 113 in water and seawater. Deep Sea Res. 42 (7), 1151–1161.

Busenberg, E., Plummer, L.N., 1992. Use of chlorofluorocarbons (CCl_3F and CCl_2F_2) as hydrologic tracers and age dating tools:

the alluvium and terrace system of Central Oklahoma. Water Resour. Res. 28 (9), 2257–2283.

Ciccioli, P., Cooper, W.T., Hammer, P.M., Hayes, J.M., 198. Organic solute–mineral surface interactions: a new method for the determination of groundwater velocities. Water Resour. Res. 16, 217–223.

Cook, P.G., Solomon, D.K., 1995. Transport of atmospheric trace gases to the water table: implications for groundwater dating with chlorofluorocarbons and krypton 85. Water Resour. Res. 31 (2), 263–270.

Cook, P.G., Solomon, D.K., 199. Recent advances in dating young groundwater: chlorofluorocarbons, $^{3}H/^{3}He$ and ^{85}Kr. J. Hydrol. 191, 245–265.

Cook, P.G., Solomon, D.K., Plummer, L.N., Busenberg, E., Schiff, S.L., 1995. Chlorofluorocarbons as tracers of groundwater transport processes in a shallow silty sand aquifer. Water Resour. Res. 31 (3), 425–434.

Craig, H., Lal, D., 1961. The production rate of natural tritium. Tellus 13, 85–105.

Dickinson, R., Cicerone, R., 1986. Future global warming from atmospheric trace gases. Nature 319, 109–115.

Dreisigacker, E., Roether, W., 1978. Tritium and ^{90}Sr in North Atlantic surface water. Earth Planet. Sci. Lett. 38, 301–312.

Dunkle-Shapiro, S., Rowe, G., Schlosser, P., Ludin, A., Stute, M., 1998. H-3/He-3 dating under complex conditions in hydraulically-stressed areas of a buried-valley aquifer. Water Resour. Res. 34, 1165–1180.

DVWK, (Deutscher Verband fuer Wasserwirtschaft und Kulturbau e.V.), 1995. Speicher-Durchfluss-Modelle zur Bewertung des Stoffein- und Stoffaustrags in unterschiedlichen Grundwasserzirkulationssystemen. Schriftenreihe des DVWK, vol. 109, p. 5.

Ekwurzel, B., Schlosser, P., Smethie, W.M.J., Plummer, L.N., Busenberg, E., Michel, R.L., Weppernig, R., Stute, M., 1994. Dating of shallow groundwater: comparison of the transient tracers $^{3}H/^{3}He$, chlorofluorocarbons, and ^{85}Kr. Water Resour. Res. 30 (6), 1693–1708.

Eriksson, E., 1963. Atmospheric tritium as a tool for the study of certain hydrologic aspects in river basins. Tellus 15, 303–308.

Fraser, P., Cunnold, D., Alyea, F., Weiss, R., Prinn, R., Simmonds, P., Miller, B., Langenfels, R., 1996. Lifetime and emission estimates of 1,1,2-trichlorotrifluoroethane (CFC-113) from daily global background observations June 1982–June 1994. J. Geophys. Res. 101 (D7), 12,585–12,599.

Friedman, H.L., 1954. The solubilities of sulfur hexafluoride in water and of the rare gases, sulfur hexafluoride and osmium tetroxide in nitromethane. J. Am. Chem. Soc. 26, 3294–3297.

Fulda, C., Kinzelbach, W., 1998. Datierungen junger Grundwässer im Gebiet Sindelfingen — Stuttgart mit Hilfe eines neuen Tracers — Schwefelhexafluorid. In: Ufrecht, W., Gerhard, E. (Eds.). Die Stuttgarter Mineralwasser — Herkunft und Genese, Stuttgart, 1. Schriftenreihe des Amts fuer Umweltschutz, Heft, pp. 139–160.

Geller, L.S., Elkins, J.W., Lobert, J.M., Clarke, A.D., Hurst, D.F., Butler, J.H., Myers, R.C., 1997. Tropospheric SF_6: observed latitudinal distribution and trends, derived emissions and interhemispheric exchange time. Geophys. Res. Lett. 24 (6), 675–678.

Gerrard, W., 1980. Gas Solubilities: Widespread Applications. Pergamon Press, New York.

Gölthenboth, J., 1997. Bestimmung von Bodenparametern in der ungesättigten Bodenzone geklüfteter Medien mit Hilfe anthropogen erzeugter Spurenstoffe.Bestimmung von Bodenparametern in der ungesättigten Bodenzone geklüfteter Medien mit Hilfe anthropogen erzeugter Spurenstoffe. Diplomarbeit, Institut für Umweltphysik, Ruprecht-Karls-Universität, Heidelberg.

Graf, W., 1995. Abschlussbericht: Begleitendes fachtechnisch-wissenschaftliches Untersuchungsprogramm zum praktischen Vollzug der Verordnung nach §29 Abs. 4 bzw. §92 Abs. 5 HWG in Verbindung mit den Verwaltungsvorschriften für die Festsetzung von Wasserschutzgebieten, GSF-Forschungszentrum für Umwelt und Gesundheit, Muenchen.

Haderlein, S.B., Schwarzenbach, R.P., 1993. Adsorption of substituted nitrobenzenes and nitrophenols to mineral surfaces. Envrion. Sci. Technol. 27 (2), 316–326.

Harnisch, J., Eisenhauer, A., 1998. Natural CF_4 and SF_6 on earth. Geophys. Res. Lett. 25, 2401.

Heaton, T.H.E., Vogel, J.C., 1981. Excess air in groundwater. J. Hydrol. 50, 201–216.

Held, J., Schuhbeck, S., Rauert, W., 1992. A simplified method of ^{85}Kr measurement for dating young groundwaters. Appl. Radiat. Isot. 43 (7), 939–942.

Hertzberg, G., 1966. Molecular Spectra and Mulecular Structure. , Vol. I: Spectra of Poyatomic Molecules. Van Nostrand Reinhold, New York.

Herzberg, O., Mazor, E., 1979. Hydrological Applications of noble gases and temperature measurements in underground water systems: examples from Israel. J. Hydrol. 41, 217–231.

HMUG, 1996. Landwirtschaft in Wasserschutzgebieten. Abschluβbericht, Hessisches Ministerium für Umwelt, Energie, Jugend, Familie und Gesundheit, Wiesbaden.

Hurst, D.F., Bakwin, P.S., Myers, R.C., Elkins, J.W., 1997. Behaviour of trace gas mixing ratios on a very tall tower in North Carolina. J. Geophys. Res. 102 (D7), 8825–8835.

Jackson, R.E., Lesage, S., Priddle, M.W., 1992. Estimating the fate and mobility of CFC-113 in groundwater: results from the Gloucester Landfill project. In: Lesage, S., Jackson, R.E. (Eds.). Groundwater Contamination and Analysis at Hazardous Waste Sites. Marcel Dekker, New York, pp. 511–526.

Katz, B.G., Lee, T.M., Plummer, N., Busenberg, E., 1995. Chemical evolution of groundwater near a sinkhole lake, northern Florida 1. Flow patterns, age of groundwater, and influence of lake water leakage. Water Resour. Res. 31 (6), 1549–1565.

Kaufman, S., Libby, W.F., 1954. The natural distribution of tritium. Phys. Rev. 93, 1337–1348.

Kinzelbach, W., 1992. Numerische Methoden zur Modellierung des Transports von Schadstoffen im Grundwasser. Oldenbourg Verlag, Munich.

Ko, M.K.W., Sze, N.D., Wang, W.-C., Shia, G., Goldman, A., Murcray, F.J., Murcray, D.G., Rinsland, C.P., 1993. Atmospheric sulfur hexafluoride: sources sinks and greenhouse warming. J. Geophys. Res. 98 (D6), 10499–10507.

Lesage, S., Jackson, R.E., Priddle, M.W., Riemann, P.G., 1990. Occurence and fate of organic solvent residues in anoxic groundwater at the Glouster landfill, Canada. Environ. Sci. Technol. 24, 559–566.

Lyman, W.J., Rheehl, W.F., Rosenblatt, D.H. (Eds.), 1982.

Handbook of Chemical and Physical Parameter Estimation McGraw-Hill, New York.

MacNeal, J.R., Rack, T.P, Corns, R.R., 1990. Process for degassing aluminium melts with sulfur hexafluoride, Patent no. 4959101, United States.

Maiss, M., 1992. Schwefelhexafluorid (SF_6) als Tracer für Mischungsprozesse im Bodensee. Inaugural-Dissertation, Ruprecht-Karls-Universität, Heidelberg, 218pp.

Maiss, M., Steele, L.P., Francey, R.J., Fraser, P.J., Langenfelds, R.L., Trivett, N.B.A., Levin, I., 1996. Sulfur hexafluoride — a powerful new amospheric tracer. Atmos. Environ. 30, 1621–1629.

Mazor, E., 1972. Paleotemperatures and other hydrological parameters deduced from noble gases dissolved in groundwaters, Jordan Rift Valley. Geochim. Cosmochim. Acta 36, 1321–1336.

McDonald, M.G., Harbaugh, A.W., 1988. A modular three dimensional finite difference groundwater flow model. USGS, Reston.

MLU, 1980. Hydrogeologische Kartierung und Grundwasserbewirtschaftung Rhein-Neckar-Raum, Ministerium für Landwirtschaft und Umwelt, Baden-Württemberg, Hessen, Rheinland-Pfalz, Stuttgart, Wiesbaden, Mainz.

Molina, M., Rowland, F.S., 1974. Stratospheric sink for chlorofluoromethanes: Chlorine atom catalyzed destruction of ozone. Nature 249, 810–812.

Montzka, S.A., Elkins, J.W., Butler, J., Thompson, T.M., Sturges, W.T., Swanson, T.H., Myers, R.C., Gilpin, T.M., Baring, T.J., Comings, S.O., Holcomb, G.A., Lobert, J.M., Hall, B.D., 1992. In: E.E. Ferguson, Rosson, R.M (Eds.), 7. Nitrous Oxide and halocarbons division. Climate monitoring and Diagnostics Laboratory, Summary report, National oceanic and atmospheric Administration, pp. 60–81.

Montzka, S.A., J, H., B, ., Myers, R.C., Thompson, T.M., Swanson, T.H., Clark, A.D., Lock, L.T., Elkins, J.W., 1996. Decline in the tropospheric abundances of halogen from halocarbons: implications for stratospheric ozone depletion. Science 272 (31), 1318–1322.

Morrison, T.J., Johnstone, N.B.B., 1955. The salting-out of non-electrolytes Part III: the inert gases and sulphur hexafluoride. J. Chem. Soc. 4, 3655–3659.

Oster, H., 1994. Datierung von Grundwasser mittels FCKW: Vorraussetzungen, Möglichkeiten und Grenzen, Inaugural-Dissertation, Ruprecht-Karls-Universität, Heidelberg, 121pp.

Oster, H., Sonntag, C., Münnich, K.O., 1996. Groundwater age dating with chlorofluorocarbons. Water Resour. Res. 32 (10), 2989–3001.

Ozima, M., Podosek, F.A., 1983. Noble Gas Chemistry. Cambridge University Press, Cambridge (367 pp.).

Plummer, L.N., Busenberg, E., Drenkard, S., Schlosser, P., McConnell, J.B., Michel, R.L., Ekwurzel, B., Weppernig, R., 1998a. Flow of river water into a karstic limestone aquifer — 2. Dating the young fraction in groundwater mixtures in the Upper Floridan Aquifer near Valdosta, Georgia. Appl. Geochem. 13, 1017–1043.

Plummer, L.N., McConnell, J.B., Busenberg, E., Drenkard, S., Schlosser, P., Michel, R.L., 1998b. Flow of river water into a karstic limestone aquifer — 1. Tracing the young fraction in groundwater mixtures in the Upper Floridan Aquifer near Valdosta, Georgia. Appl. Geochem. 13, 995–1015.

Rath, H.K., 1988. Simulation der globalen ^{85}Kr und $^{14}CO_2$ Verteilung mit Hilfe eines zeitabhängigen, zweidimensionalen Modells der Atmosphäre. Dissertation, Ruprecht-Karls-Universität, Heidelberg, 89 pp.

Ravishankara, A.R., Solomon, S., Turnipseed, A.A., Warren, R.F., 1993. Atmospheric lifetimes of long-lived halogenated species. Science 259, 194–199.

Roy, W.R., Griffin, R.A., 1985. Mobility of Organic solvents in water-saturated soil materials. Environ. Geol. Water Sci. 7 (4), 241–247.

Rózanski, K., Florkowski, T., 1979. Krypton-85 dating of groundwaters. Isotope Hydrology. International Atomic Energy Agency, Vienna, pp. 949–961.

Rudolph, J., Rath, H.K., Sonntag, C., 1983. Noble gases and stable isotopes in ^{14}C dated paleowaters from Central Europe and the Sahara. Isotope Hydrology. International Atomic Energy Agency, Vienna, pp. 467–477.

Rupp, H., 1993. Parametrisierung eines massenspektrometrischen Meßsystems zur Neonmessung und Untersuchung der He/Ne-Verhältnisse in hydrothermalen Fluiden. Dissertation, Ruprecht-Karl-Unversität Heidelberg, Heidelberg, 128 pp.

Schröder, K.J.P., Roether, W., 1975. The releases of krypton-85 and tritium to the environment and tritium to krypton-85 ratios as source indicators. Isotope Ratios as Pollutant Source and Behaviour Iindicators. International Atomic Energy Agency, Vienna, pp. 231–253.

Schwarzenbach, R.P., Westall, J., 1981. Transport of nonpolar organic compounds from surface water to groundwater. Environ. Sci. Technol 15 (11), 1360–1367.

Schwarzenbach, R.P., Gschwend, P.M., Imboden, D.M., 1993. Environmental Organic Chemistry. Wiley, New york.

Seelmann-Eggebert, W., Pfennig, G., Münzel, H. and Klewe-Nebenius, H., 1981. Nuklidkarte, Kernforschungszentrum Karlsruhe, Karlsruhe, 32 p.

Simmonds, P.G., Cunnold, D.M., Dollard, G.J., Davies, T.J., McCulloch, A., Derwent, R.G., 1992. Evidence of phase out of CFC use in Europe over the period 1987–1990. Atmos. Environ. 27A, 1397–1407.

Singh, H.B., Salas, L., Viezee, W., Sitton, B., Ferek, R., 1992. Measurement of volatile organic chemicals at selected sites in California. Atmos. Environ. 26A, 2929–2946.

Singh, H.B., Salas, L.J., Cavanagh, L.A., 1977. Distribution, sources and sinks of atmospheric halogenated compounds. . J. Air Pollut. Control. Assoc. 27, 333–336.

Singh, H.B., Salas, L.J., Stiles, R.E., 1983. Selected man-made halogenated chemicals in the air and oceanic environment. J. Geophys. Res. 88 (C6), 3675–3683.

Sittkus, A., Stockburger, H., 1976. Krypton-85 als Indikator des Kernbrennstoffverbrauchs. Naturwissenschaften 63, 266–272.

Smethie, W.M., Solomon, D.K., Shiff, S.L., Mathieu, G.G., 1992. Tracing groundwater flow in the Borden aquifer using krypton-85. J. Hydrol. 130, 279–297.

Solvay, 1994. Schwefelhexafluorid, Produktbeschreibung. 39/101/01.94/007/3000, Solvay Fluor und Derivate GmbH, Hannover.

Sontheimer, H., Cornel, P., Seym, M., 1983. Untersuchung zur

Sorption von aliphatischen Chlorkohlenwasserstoffen durch Boeden aus GRundwasserleitern, vol. 21. Mitteilungen des Engler-Bunte Instituts, Karlsruhe, Germany, pp. 1–46.

Stordal, F., Innset, B., Grossman, A.S., Myrhe, G., 1993. SF_6 as a greenhouse gas: an assessment of Norwegian and global sources and the global warming potential. NILU-Report, OR 15/93, O-92102, Norsk institutt for luftforskning, Kjeller.

Stute, M., 1989. Edelgase im Grundwasser — Bestimmung von Paläotemperatuten und Untersuchung der Dynamik von Grundwasserfließsystemen. Inaugural-Dissertation, Ruprecht-Karls-Universität, Heidelberg, 138 pp.

Szabo, Z., Rice, D.E., Plummer, L.N., Busenberg, E., Drenkard, S., Schlosser, P., 1996. Age dating of shallow groundwater with chlorofluorocarbons, tritium/helium 3, and flow path analysis, southern New Jersey coastal plain. Water Resour. Res. 32 (4), 1023–1038.

Thompson, G.M., Hayes, J.M., 1979. Trichlorflouromethane in groundwater — a possible tracer and indicator of groundwater age. Water Resour. Res. 15 (3), 546–554.

Tominaga, T., 1992. Chlorofluorocarbons in the atmosphere: trends and vertical profiles. Pure Appl. Chem. 64 (4), 529–536.

Unterweger, M.P., Corusey, B.M., Schima, F.J., Mann, W.B., 1980. Preparation and calibration of the National Bureau of Standards tritiated-water standards. Int. J. Appl. Radiat. Isot. 31, 611–614.

Vassolo, S., 1995. Berechnung von Brunneneinzugsgebieten mit Hilfe stochastischer Methoden. Dissertation zur Erlangung des Grades eines Doktor-Ingenieurs, Universität-Gesamthochschule, Kassel, 134 pp.

Vassolo, S., Kinzelbach, W., Schäfer, W., 1998. Determination of a well head protection zone by stochastic inverse modelling. J. Hydrol. 206 (3–4), 268–280.

Wanninkhof, R., Ledwell, J.R., Watson, A.J., 1991. Analysis of sulfur hexafluoride in seawater. J. Geophys. Res. 96 (C5), 8733–8740.

Watson, A.J., Liddicoat, M.I., 1985. Recent history of atmospheric trace gas concentrations deduced from measurements in the deep sea: application to sulphur hexaflouride and carbon tetrachloride. Atmos. Environ. 19 (9), 1477–1484.

Weiss, R.F., 1971. Solubility of helium and neon in water and seawater. J. Chem. Engng Data 16 (2), 235–241.

Weiss, W., Sartorius, H., Stockburger, H., 1992. Global distribution of atmospheric ^{85}Kr. Isotopes of Noble Gases as Tracers in Environmental Studies. International Atomic Energy Agency, Vienna, pp. 29–62.

Wilhelm, E., Battino, R., Wilcock, R.J., 1977. Low-pressure solubility of gases in liquid water. Chem. Rev. 77 (2), 219–256.

WMO, 1988. The Montreal Protocol on substances that deplete the ozone layer. WMO Bull. 37, 94–97.

Zheng, C., 1990. MT3D, A modular three-dimensional transport model. S.S. Papadopulos & Associates, Rockville, Maryland.

Zoellmann, K.P., Kinzelbach, W., 1996. Use of a numerical flow and transport model in the interpretation of environmental tracer data. ModelCARE 96. In: International Conference on Calibration and Reliability in Groundwater Modelling, Colorado School of Mines Golden, Colorado, USA, pp. 371–379.

Zoellmann, K.P., Kinzelbach, W., Fulda, C., 2001. Environmental tracer transport (3H and SF6) in the saturated and unsaturated zones and its use in nitrate pollution management. J. Hydrol. 240, 187–205.